

Sergey A. Lebedev



*Geophysical Center,
Russian Academy of Sciences*



*Space Research Institute,
Russian Academy of Sciences*

Satellite altimetry: History and Method



Joint COSPAR and WMO Capacity Building Workshop
«Satellite remote sensing, water cycle and climate change»

© 2014, S.A. Lebedev, GC RAS, SRI RAS



20 July — 1 August 2014,
Tver, Russian Federation
Tver State University



Altimeter

An altimeter or an altitude meter is an instrument used to measure the altitude of an object above a fixed level. The measurement of altitude is called altimetry, which is related to the term bathymetry, the measurement of depth underwater.

On the principle of the device is divided into
Pressure altimeter and Radar altimeter.



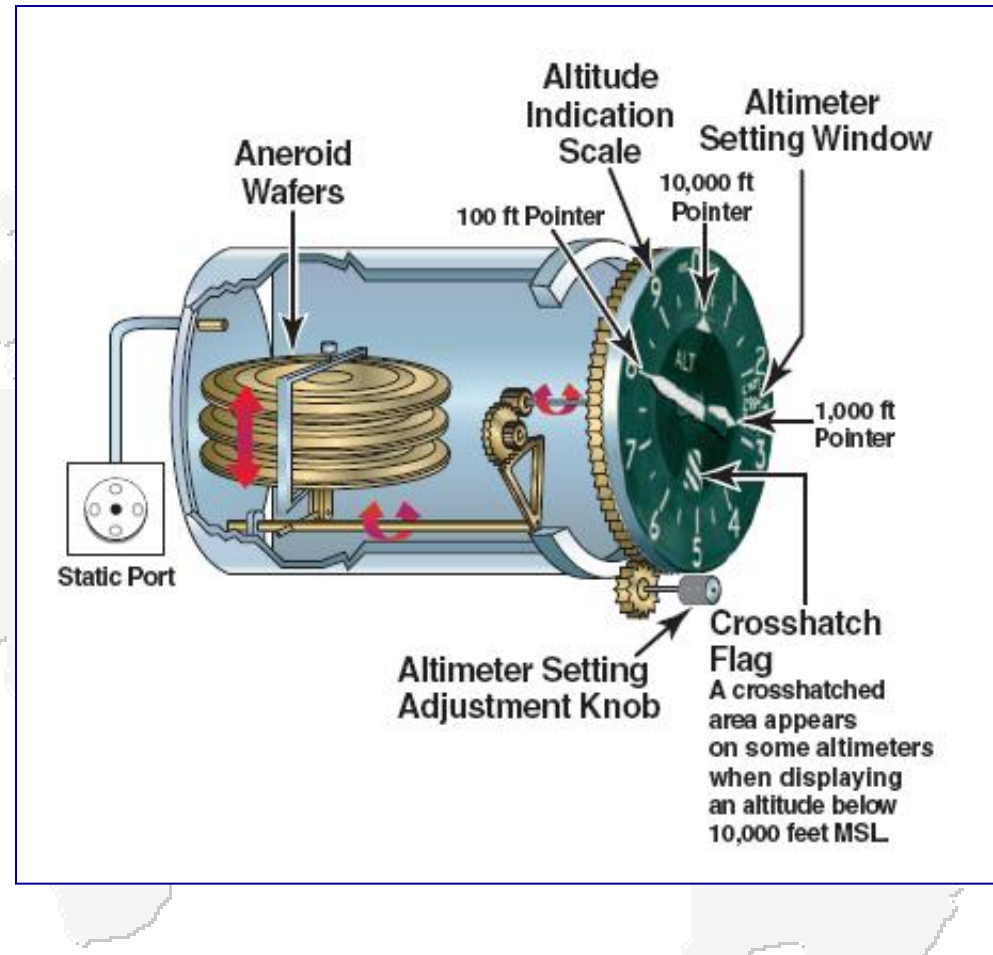
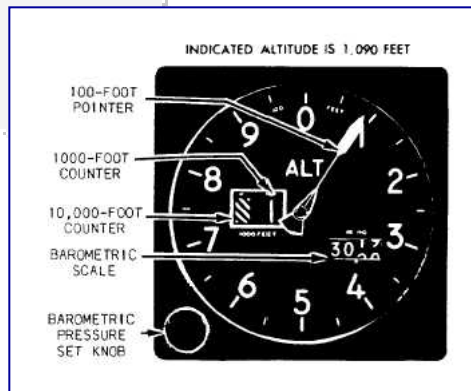
Pointer Pressure altimeter in an airplane cockpit



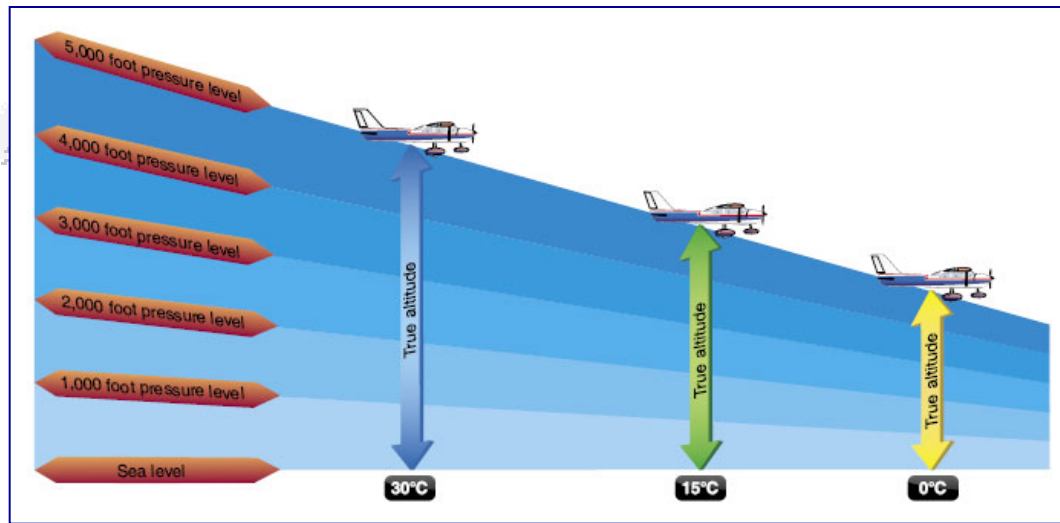
Pointer Radar altimeter in an airplane cockpit

Pressure Altimeter

Altitude can be determined based on the measurement of atmospheric pressure. The greater the altitude the lower the pressure. A pressure altimeter is the altimeter found in most aircraft, and skydivers use wrist-mounted versions for similar purposes.



Pressure Altimeter



Reported Temp 0 °C	Height Above Airport in Feet														
	200	300	400	500	600	700	800	900	1000	1500	2000	3000	4000	5000	
+10	10	10	10	10	20	20	20	20	20	30	40	60	80	90	
0	20	20	30	30	40	40	50	50	60	90	120	170	230	280	
-10	20	30	40	50	60	70	80	90	100	150	200	290	390	490	
-20	30	50	60	70	90	100	120	130	140	210	280	420	570	710	
-30	40	60	80	100	120	140	150	170	190	280	380	570	760	950	
-40	50	80	100	120	150	170	190	220	240	360	480	720	970	1210	
-50	60	90	120	150	180	210	240	270	300	450	590	890	1190	1500	

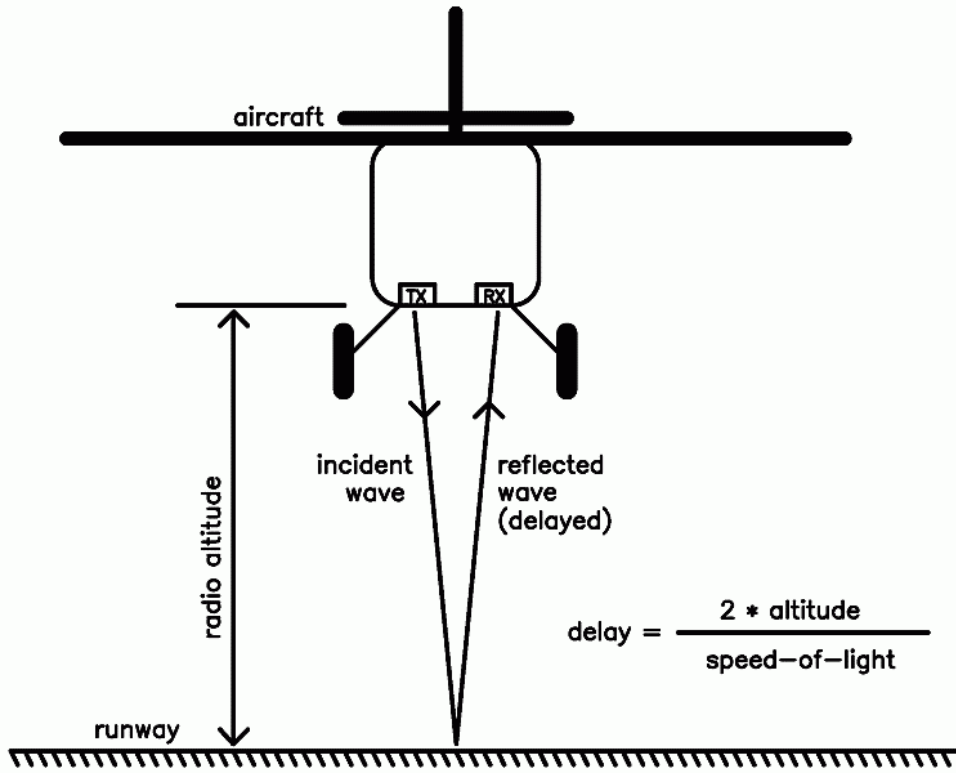
The calibration of an pressure altimeter follows the equation

$$z = c T \log(P_0/P)$$

where c is a constant, T is the absolute temperature, P is the pressure at altitude z , and P_0 is the pressure at sea level. The constant c depends on the acceleration of gravity and the molar mass of the air.



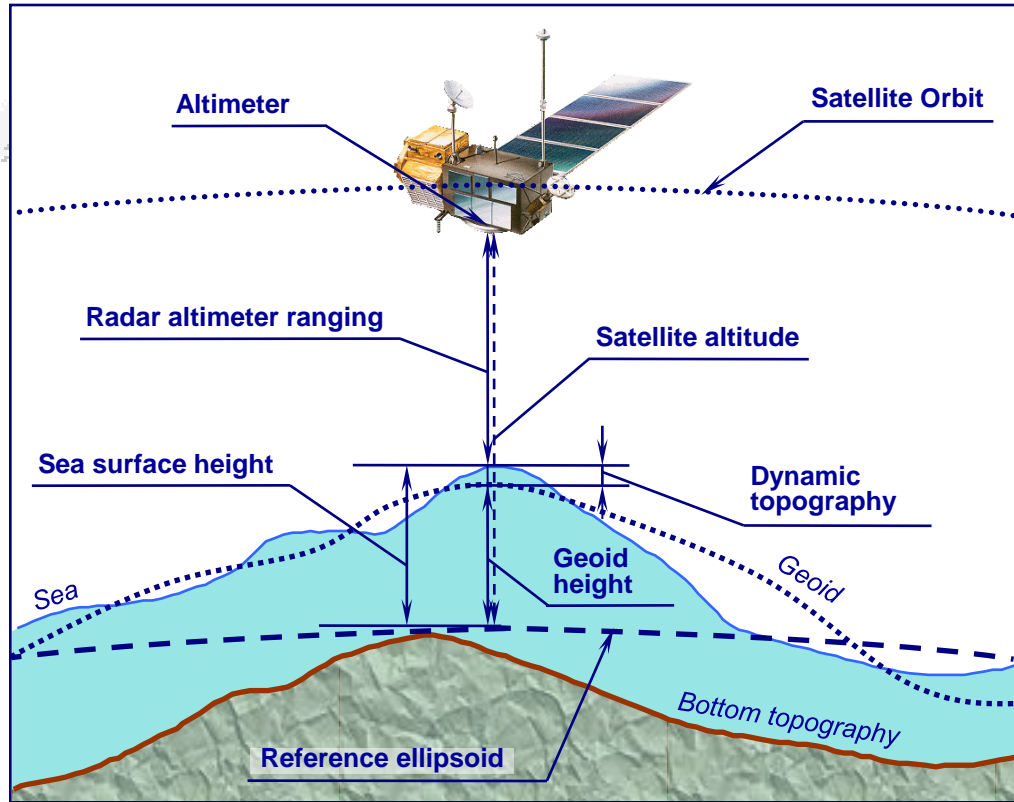
Radar Altimeter



A radar altimeter measures altitude more directly, using the time taken for a radio signal to reflect from the surface back to the aircraft. The radar altimeter is used to measure height above ground level during landing in commercial and military aircraft.



Basic Principle of Satellite Altimetry



Satellite altimetry allows us to analyze:

- amplitude of the wind speed
- significant wave height
- state of the underlying surface

H_g – geoid height the or height of the Earth's gravitational field equipotential surface

H_{orb} – satellite orbit height

H_{alt} – radar altimeter ranging

H_{ssh} – sea surface height based on correction (dH_i), atmospheric refraction (dry gases, water vapour, ionospheric electrons), instrument error and sea state bias:

$$H_{ssh} = H_{orb} - H_{alt} - \sum dH_i$$

H_{dt} – dynamic topography or deviation of the sea surface height relative to the geoid height : $H_{dt} = H_{ssh} - H_g$



Joint COSPAR and WMO Capacity Building Workshop
«Satellite remote sensing, water cycle and climate change»

© 2014, S.A. Lebedev, GC RAS, SRI RAS

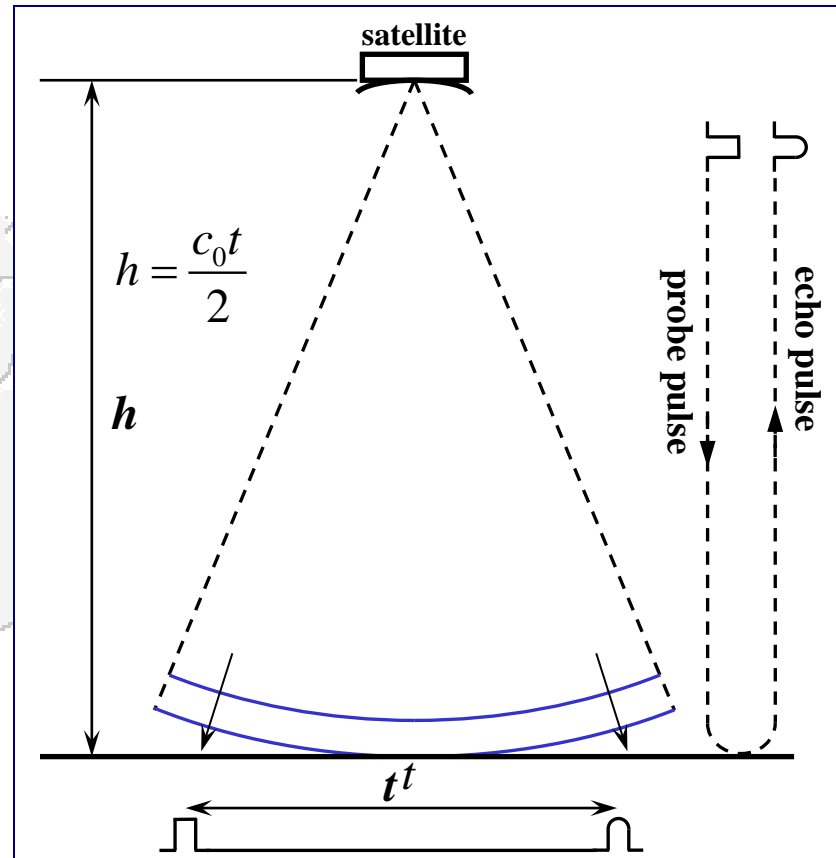


20 July — 1 August 2014,
Tver, Russian Federation
Tver State University.



Satellite Altimeter

Altimetry satellites basically determine the distance from the satellite to a target surface by measuring the satellite-to-surface round-trip time of a radar pulse. However, this is not the only measurement made in the process, and a lot of other information can be extracted from altimetry.



Schematic diagram of the altimeter work



Joint COSPAR and WMO Capacity Building Workshop
«Satellite remote sensing, water cycle and climate change»

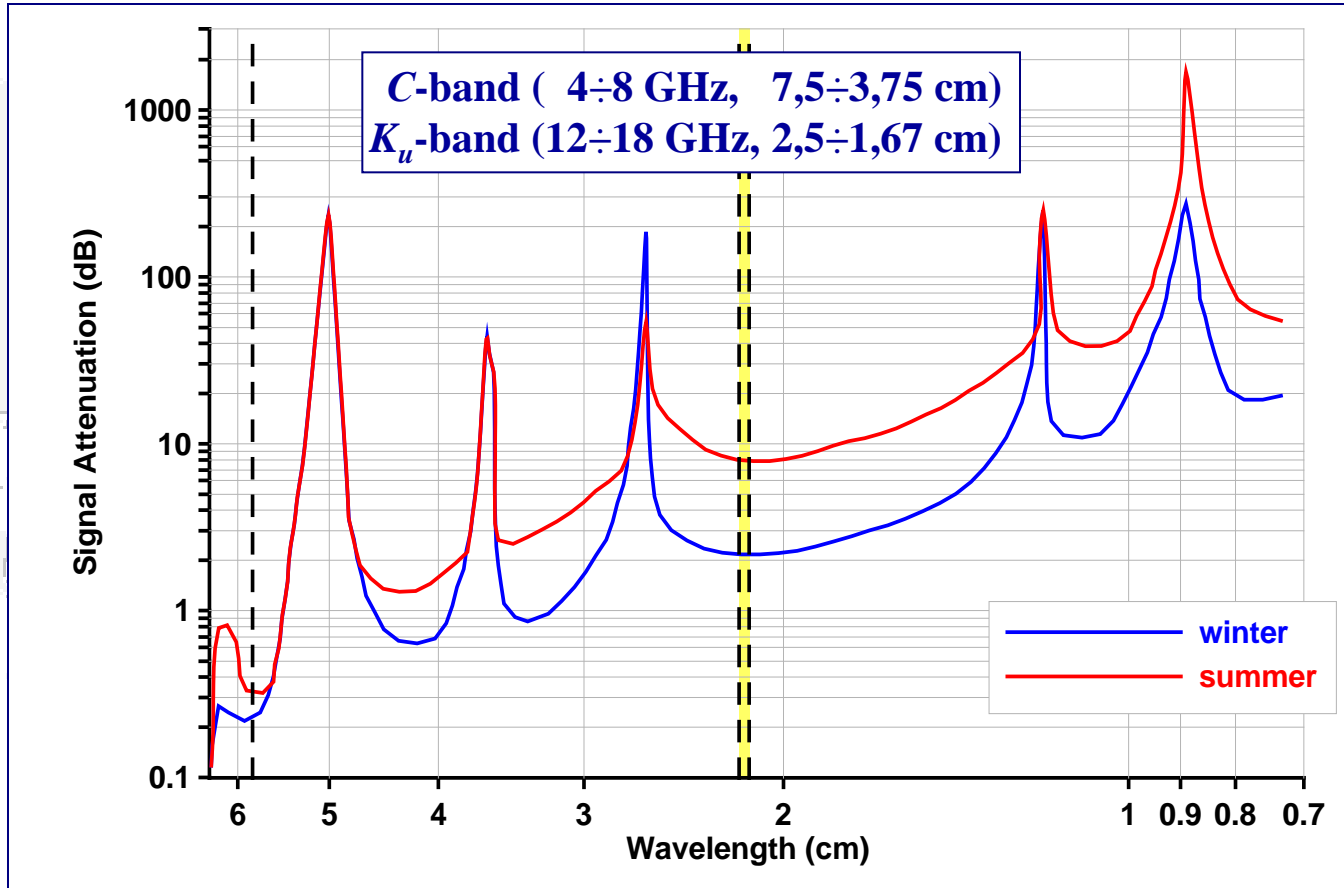
© 2014, S.A. Lebedev, GC RAS, SRI RAS



20 July — 1 August 2014,
Tver, Russian Federation
Tver State University



Operating Frequency Altimeter



Frequency-dependent attenuation of electromagnetic radiation in standard atmosphere.
The vertical dotted lines indicate the wavelengths and operating frequencies and yellow wavelength range and operating frequency of modern altimeters



Joint COSPAR and WMO Capacity Building Workshop
«Satellite remote sensing, water cycle and climate change»

© 2014, S.A. Lebedev, GC RAS, SRI RAS

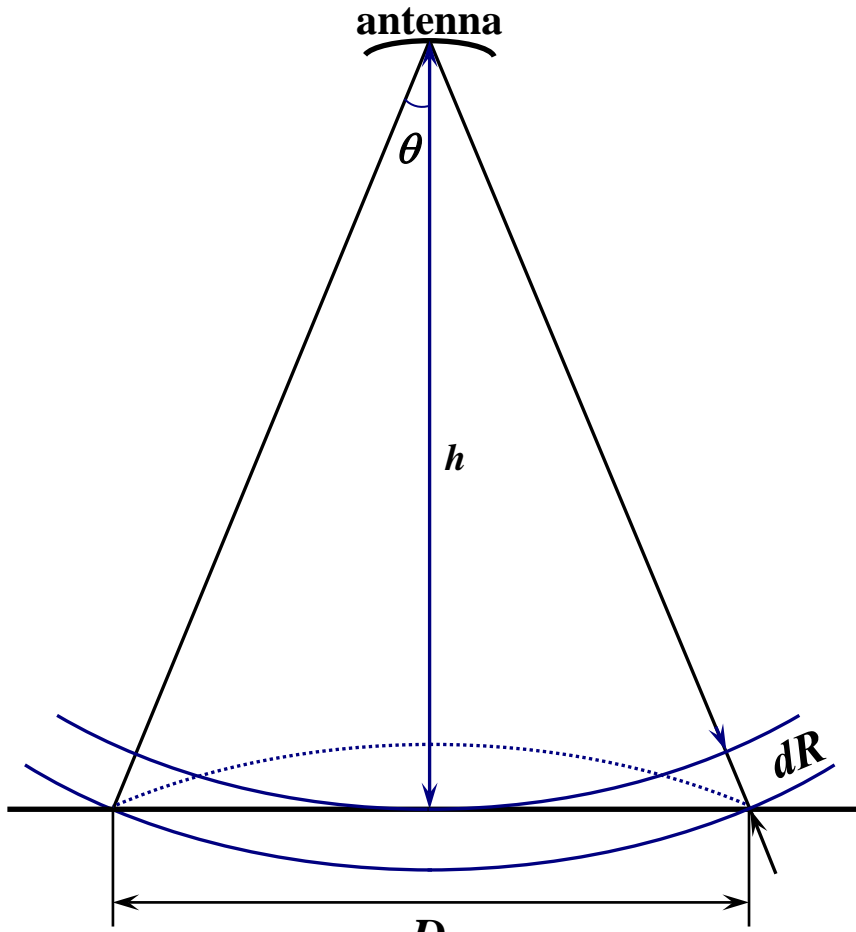


20 July — 1 August 2014,
Tver, Russian Federation
Tver State University.



Pulse-limited Footprint

Schematic diagram showing the configuration when the trailing edge of the pulse arrives at the flat ocean surface



$$D_s = 2\sqrt{2h\Delta R} = 2\sqrt{2hc\tau}$$



Joint COSPAR and WMO Capacity Building Workshop
«Satellite remote sensing, water cycle and climate change»

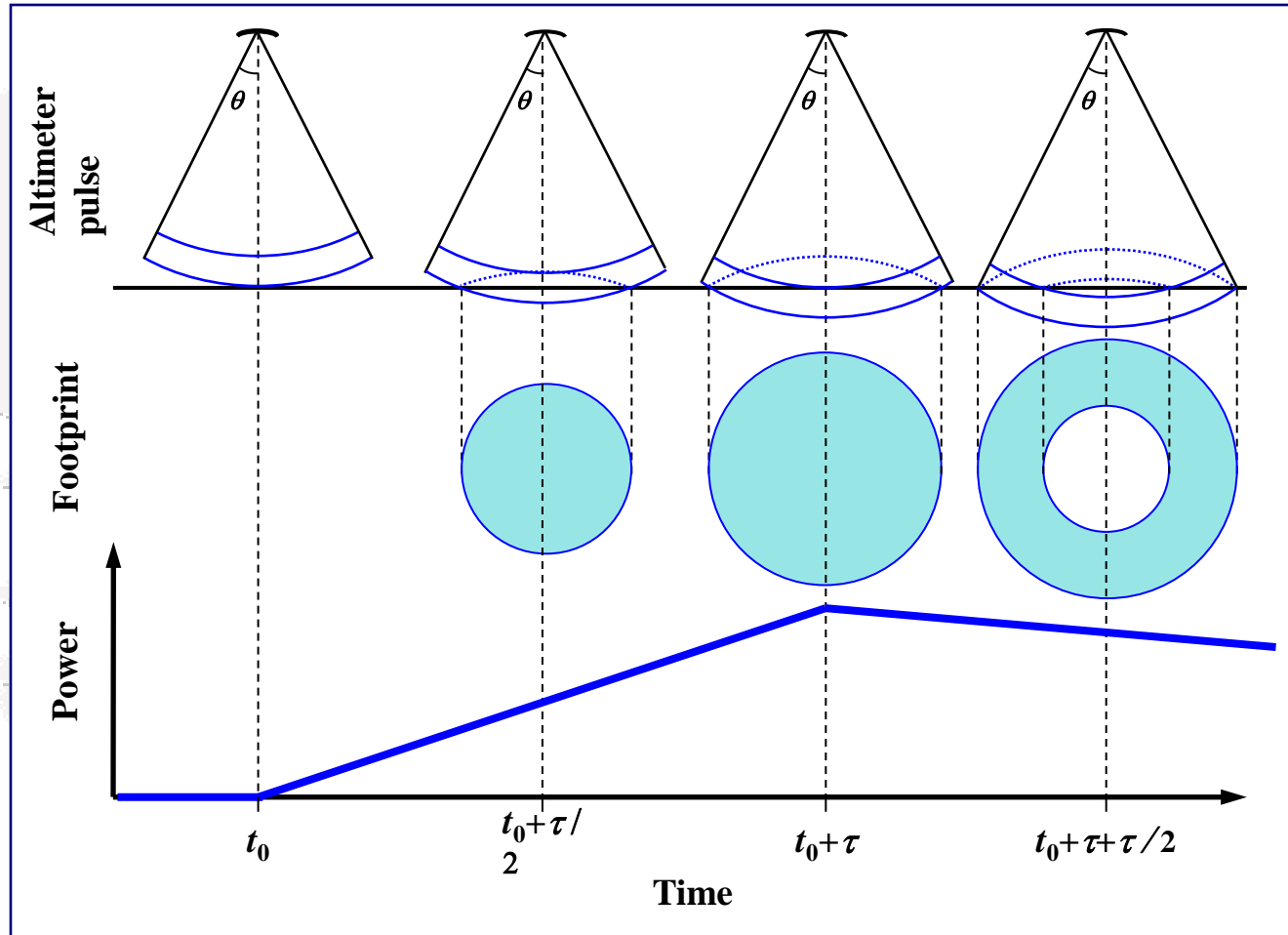
© 2014, S.A. Lebedev, GC RAS, SRI RAS



20 July — 1 August 2014,
Tver, Russian Federation
Tver State University.



Altimeter Footprint Size



Schematic representation of a wide beam width, short pulse propagation from the satellite to the sea surface (upper row). The antenna footprint on the sea surface is shown as a function of time in the middle row. The area of the footprint is shown as a function of time in the bottom panel.



Joint COSPAR and WMO Capacity Building Workshop
«Satellite remote sensing, water cycle and climate change»

© 2014, S.A. Lebedev, GC RAS, SRI RAS

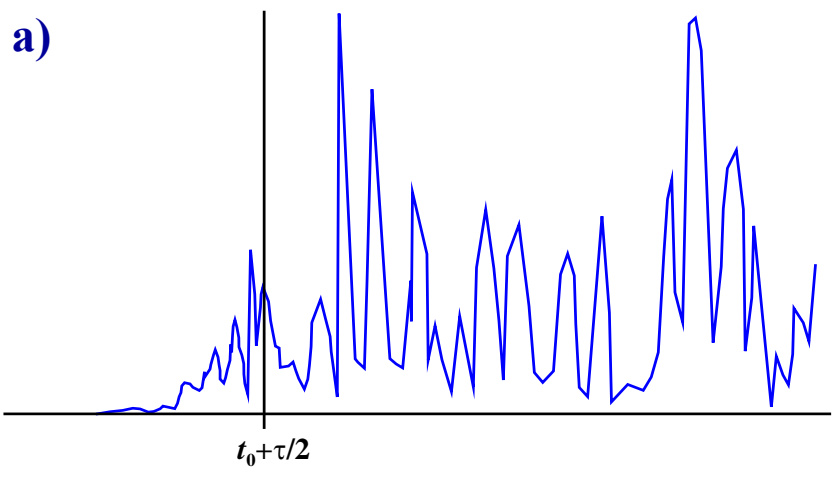


20 July — 1 August 2014,
Tver, Russian Federation
Tver State University

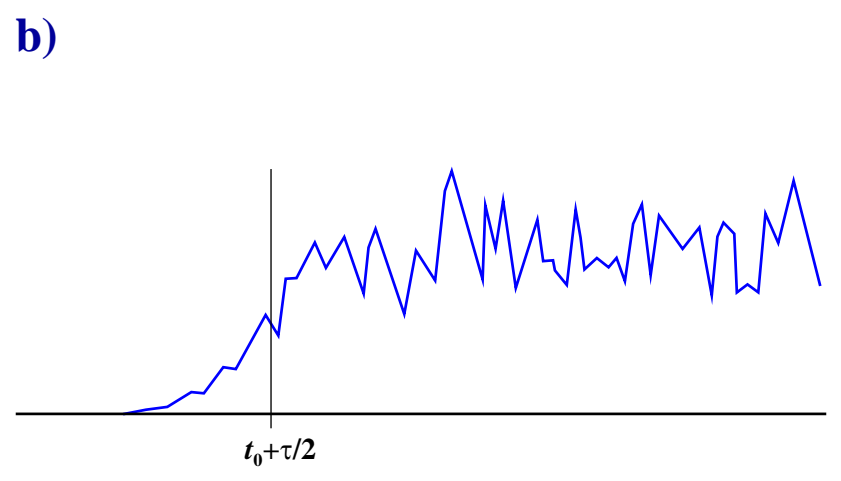


Averages of Form Pulse

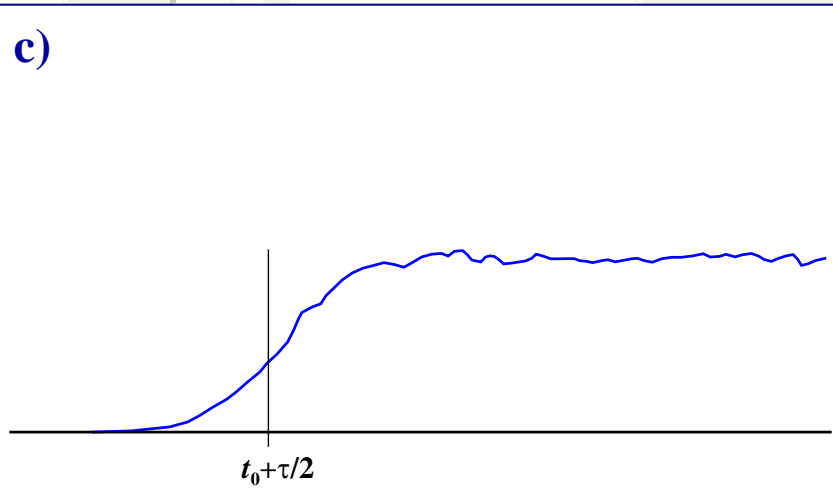
a)



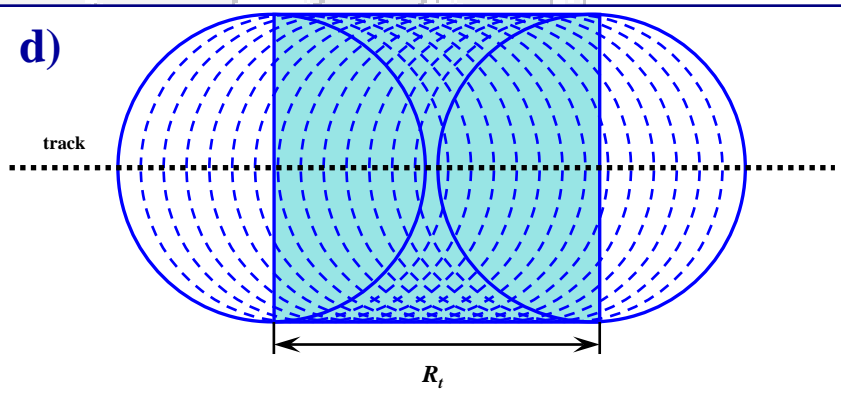
b)



c)



d)



Averages of 1 (a), 25 (b), and 1000 (c) simulated independent time series and illuminated footprint size.



Joint COSPAR and WMO Capacity Building Workshop
«Satellite remote sensing, water cycle and climate change»

© 2014, S.A. Lebedev, GC RAS, SRI RAS



20 July — 1 August 2014,
Tver, Russian Federation
Tver State University



Echo Waveforms Characteristics

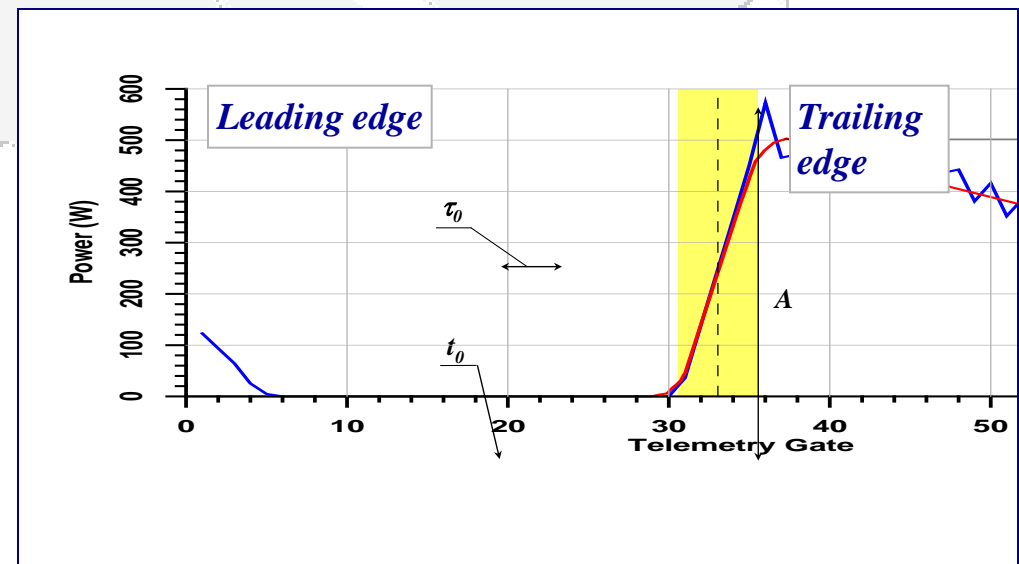
Average echo form of pulse reflected from the sea surface which are received altimeter

$$P(t) = P_{FS}(t) * s_r(t) * q_s(t)$$

- $P_{FS}(t)$ – the average power of the signal reflected by a flat surface
 $s_r(t)$ – the form of the pulse reflected from the flat surface
 $q_s(t)$ – the probability density distribution of the heights of the reflection points
* – convolution operator

Theoretical form of the echo pulse for an infinite underlying surface and one-second averaged form of the echo pulse for the conditions of the open ocean (blue line).

Yellow highlighted area width of rise-up portion of the echo pulse.



Joint COSPAR and WMO Capacity Building Workshop
«Satellite remote sensing, water cycle and climate change»

© 2014, S.A. Lebedev, GC RAS, SRI RAS



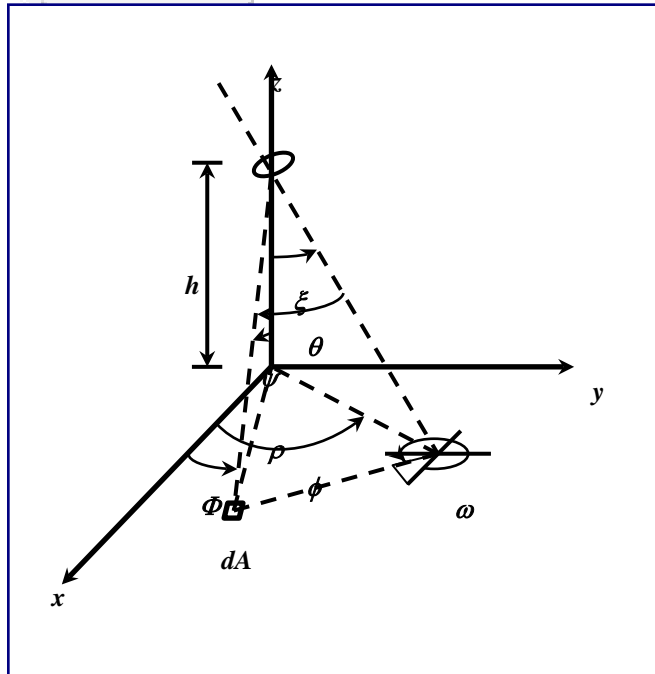
20 July — 1 August 2014,
Tver, Russian Federation
Tver State University.



Theoretical Bases of Satellite Altimetry

Brown formula:

$$P_i(t) = P_0 \iint_{\text{illuminated area}} \frac{G^2(\theta)\sigma(x, y, \theta)}{r^4} dA \int_{-\infty}^{\infty} p\left(t_1 - \frac{2r}{c}\right) q\left(x, y, \frac{c}{2}(t - t_1)\right) dt_1$$



- G – antenna directional diagram
 r – the distance from the antenna to the elementary area dA on the surface
 $p(t)$ – the shape of the emitted impulse
 h – the mean distance from the satellite to the surface
 σ – the scattering cross-section per unit area
 $q(z)$ – the probability density of the height of mirror (scattering) points



Joint COSPAR and WMO Capacity Building Workshop
«Satellite remote sensing, water cycle and climate change»

© 2014, S.A. Lebedev, GC RAS, SRI RAS



20 July — 1 August 2014,
Tver, Russian Federation
Tver State University.



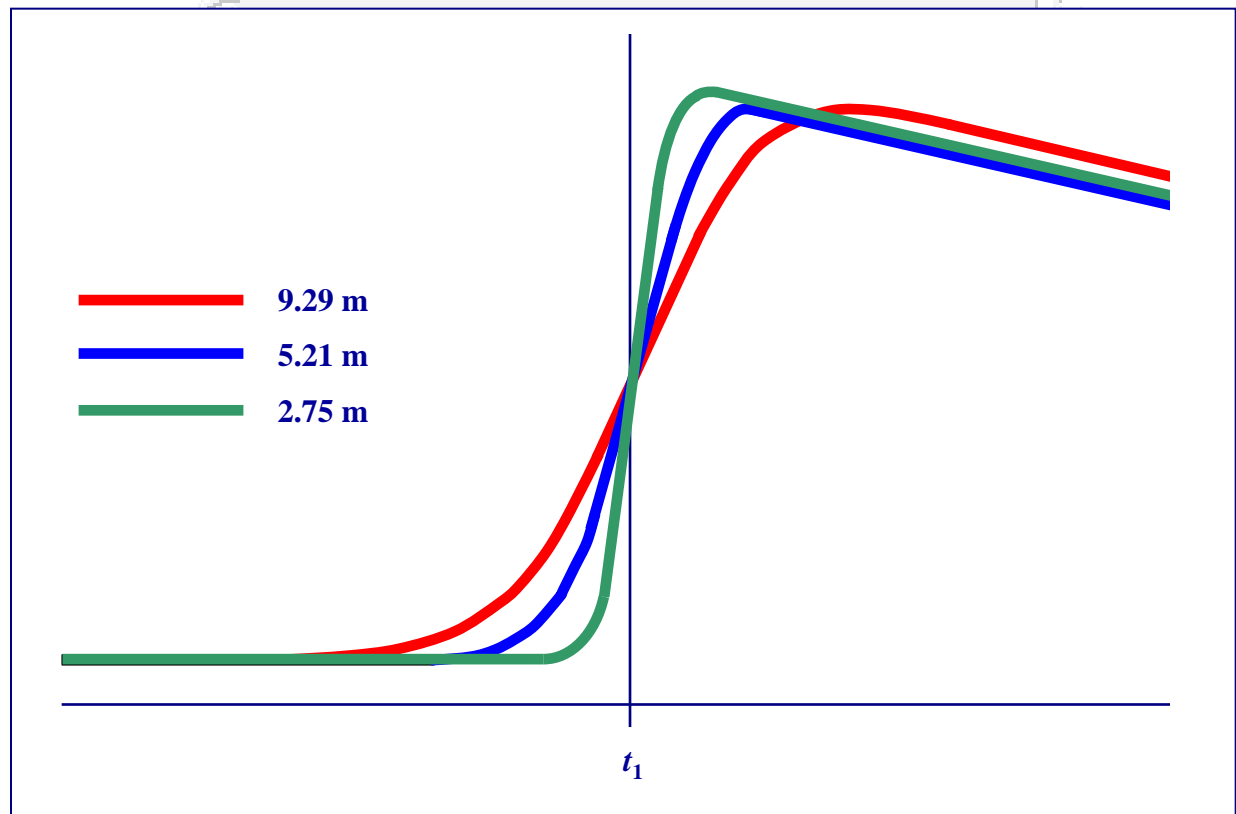
Significant Wave Height

Average echo form of pulse reflected from the sea surface which are received altimeter

$$P(t) = P_{FS}(t) * s_r(t) * q_s(t)$$

$q_s(t)$ – the probability density distribution of the heights of the reflection points

Examples of theoretical echo forms reflected pulse to different SWH



Joint COSPAR and WMO Capacity Building Workshop
«Satellite remote sensing, water cycle and climate change»

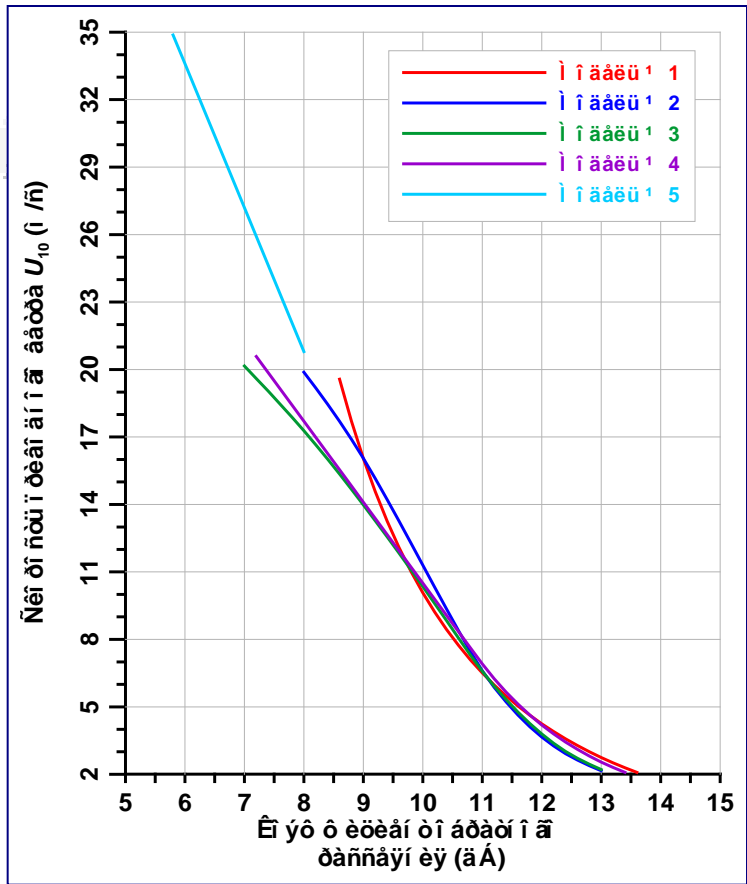
© 2014, S.A. Lebedev, GC RAS, SRI RAS



20 July — 1 August 2014,
Tver, Russian Federation
Tver State University



Wind Speed



Wind speed dependence of the backscattering coefficient

1. Brown (1979):

$$U_{10} = \exp \left[\left(10^{-(0,21+\sigma^0/10)} - B \right) / A \right]$$

2. Chelton & McCabe (1985):

$$U_{10} = 0,943 \cdot 10^{[(\sigma^0/10-A)/B]}$$

3. Witter &Chelton (1991):

$$U_{10} = \sum_{n=0}^5 A_n (\sigma^0)^n$$

4. Abdalla (2012):

$$U_{10} = \begin{cases} A_1 - B_1 \sigma^0 \\ A_2 \exp(-B_2 \sigma^0) \end{cases}$$

5. Young (1993):

$$U_{10} = A \sigma^0 + B$$

Error Budget

- ⇒ Dry Troposphere correction (2–3 m) - Refraction from the dry gas component of the atmosphere create a signal delay in the radar.

$$dh_{dry} = 2,277 \cdot P_{surf} \left(1 + 0,0026 \cos(2\phi) \right)$$

- ⇒ Wet Troposphere correction (<0.5 m) - Water vapor can also cause a delay in the radar signal which can be more difficult to correct. A delay correction for the total water column in the radar measurement can be accounted for using output from meteorological models, like ECMWF and NCEP.

$$dh_{wet} = - \left(1,11645410^{-3} \int_{P_{sat}}^{P_{surf}} q \, dP + 17,66543928 \int_{P_{sat}}^{P_{surf}} \frac{q}{T} \, dP \right) (1 + 0,0026 \cos(\phi))$$

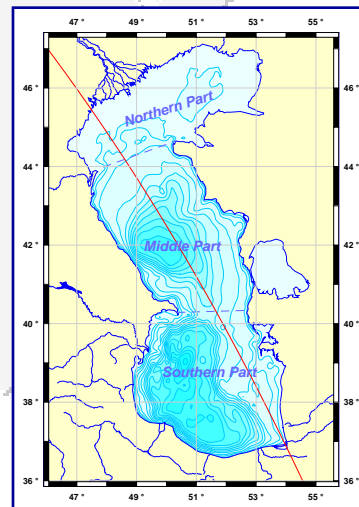
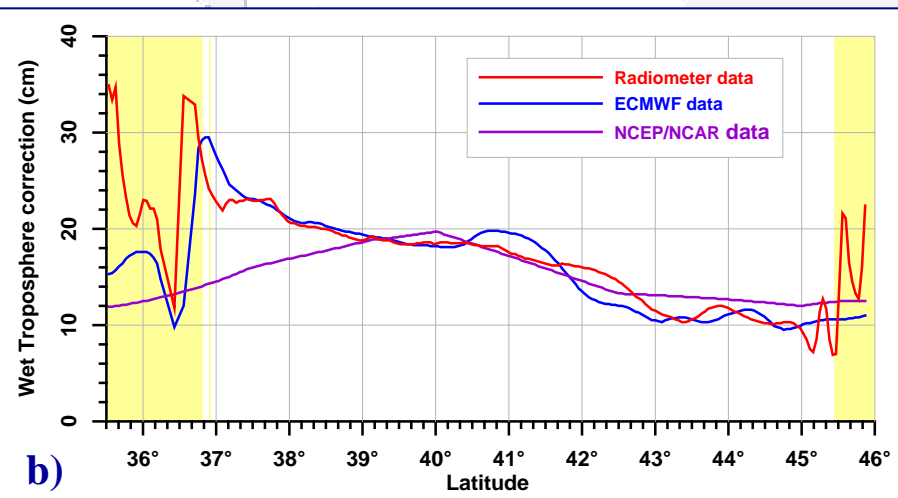
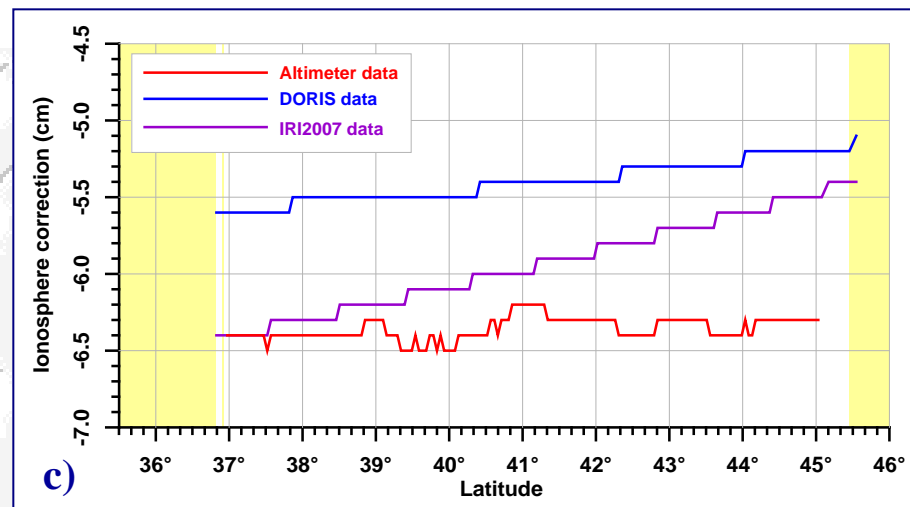
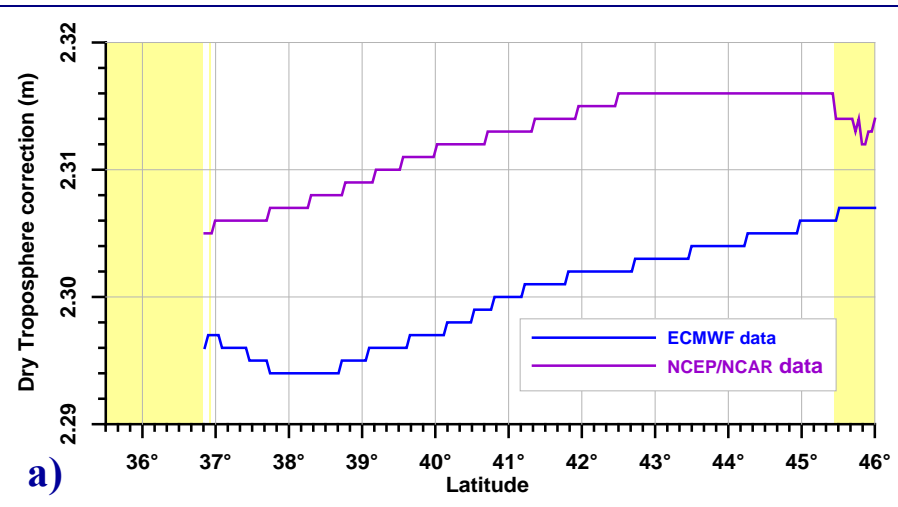
or

$$dh_{wet} = \beta_0 + \sum_{i=1}^N \beta_i \ln(280 - T_{Bi})$$

- ⇒ Ionosphere correction (0.02-0.2 m) - The ionosphere can also impose a delay on the radar return signal, where electron plasma in the ionosphere slow down the group velocity of the radar pulse. The electron density in the ionosphere varies throughout the day, complicating the ionosphere correction.



Error Budget



Variability of dry (a) and wet (b) troposphere corrections and ionosphere correction (c) along the track 092 satellites Jason-2 on August 1, 2012 (150 cycle) on the Caspian Sea area (d).



Error Budget

- ⇒ Electromagnetic Bias (0.02-0.05 m) - There is a sea state bias where the troughs of waves tend to focus waves back to the radar, while the crests of the waves scatter waves away from nadir.

$$dh_{emb} = F_1(h_{swh}, U_{10}) \approx F_1(h_{swh}, \sigma^0)$$

- ⇒ Inverse barometer correction

$$dh_{inv} = -9,948(P_s - P_0)$$

- ⇒ Tides - Tidal variations are much larger than the dynamic variations in sea surface height. Because tidal periods can be on the order of diurnal and semidiurnal, the tides create an aliased frequency in the temporal variations in the sea level height that must be removed.



Joint COSPAR and WMO Capacity Building Workshop
«Satellite remote sensing, water cycle and climate change»

© 2014, S.A. Lebedev, GC RAS, SRI RAS



20 July — 1 August 2014,
Tver, Russian Federation
Tver State University.



History of radar altimeters

Satellite	Period of active work month/year	mass, kg	Orbit parameter				
			Altitude, perigee	apogee	inclination, degree	Exact repeat cycle ² , day	
Skylab-4 (орбитальная станция)	05/1973 – 02/1974	20847	422	437	130	–	
GEOS-3	04/1978 – 12/1978	341	817	858	115	–	
SEASAT	07/1978 – 09/1978	2300	761	765	108	17	
	09/1978 – 10/1978					3	
GEOSAT	геодезическая программа	03/1985 – 11/1986	635	775	779	108,1	
	изомаршрутная программа	11/1986 – 12/1989					
GEOIK 1 ¹	07/1985 – 10/1986	1500	1482	1525	73,6	–	
GEOIK 2 ¹	03/1986 – 03/1986	1500	1480	1525	73,6	–	
GEOIK 3 ¹	12/1986 – 12/1987	1500	1497	1504	82,6	–	
GEOIK 4 ¹	03/1987 – 10/1987	1500	1479	1524	73,6	–	
GEOIK 5 ¹	06/1988 – 07/1990	1500	1484	1522	73,6	–	
GEOIK 6 ¹	09/1989 – 09/1990	1500	1485	1524	73,6	–	
GEOIK 7 ¹	08/1990 – 03/1993	1500	1484	1524	73,6	–	
ERS-1	Фазы А, В	07/1991 – 03/1992	2384	774	775	98,5	
	Фаза С	04/1992 – 12/1993					
	Фаза D	12/1993 – 04/1994					
	Фазы Е ¹ , F ¹	04/1994 – 03/1995					
	Фаза G	04/1995 – 06/1996					
TOPEX/ Poseidon	Фаза А	08/1992 – 08/2002	2402	1331	1344	66,04	
	Фаза В	09/2002 – 01/2006					
GEOIK 8 ¹	01/1993 – 07/1993	1500	1479	1525	73,6	–	
GEOIK 9 ¹	12/1994 – 07/1995	1500	1481	1526	73,6	–	
ERS-2	04/1995 – 06/2002	2516	784	785	98,6	35	
GFO-1	02/1998 – 10/2008	410	786	788	108,1	17	
Jason-1	Фаза А	12/2001 – 01/2009	500	1337	1343	66,2	
	Фаза В	02/2009 – 02/2012				66,042	
	Фаза С ¹	05/2012 – 07/2013				~406	
ENVISAT	03/2002 – 04/2012	7991	783	785	98,6	35	
ICESat	01/2003 – настоящее время	1000	593	610	94	183,8	
CryoSat-1	08.10.2005 – потерян при выводе на орбиту	650	720		92	~369	
OSTM/Jason-2	06/2008 – настоящее время	510	1324	1335	66,04	10	
CryoSat-2	04/2010 – настоящее время	720	717		92,0	~369	
HaiYang-2A (HY-2A)	изомаршрутная программа	08/2011 – настоящее время	513	963,6	965	99,3	
	геодезическая программа						
CAJIKO (Poseidon-2)	12/2011 - ошибка вывода на орбиту	1500	1347		73,6	17	
SARAL/Altika	02/2013 – настоящее время	450	786		98,705	35	

¹ – Geodetic mission

² – Exact Repeat Mission

Joint COSPAR and WMO Capacity Building Workshop
«Satellite remote sensing, water cycle and climate change»

© 2014, S.A. Lebedev, GC RAS, SRI RAS

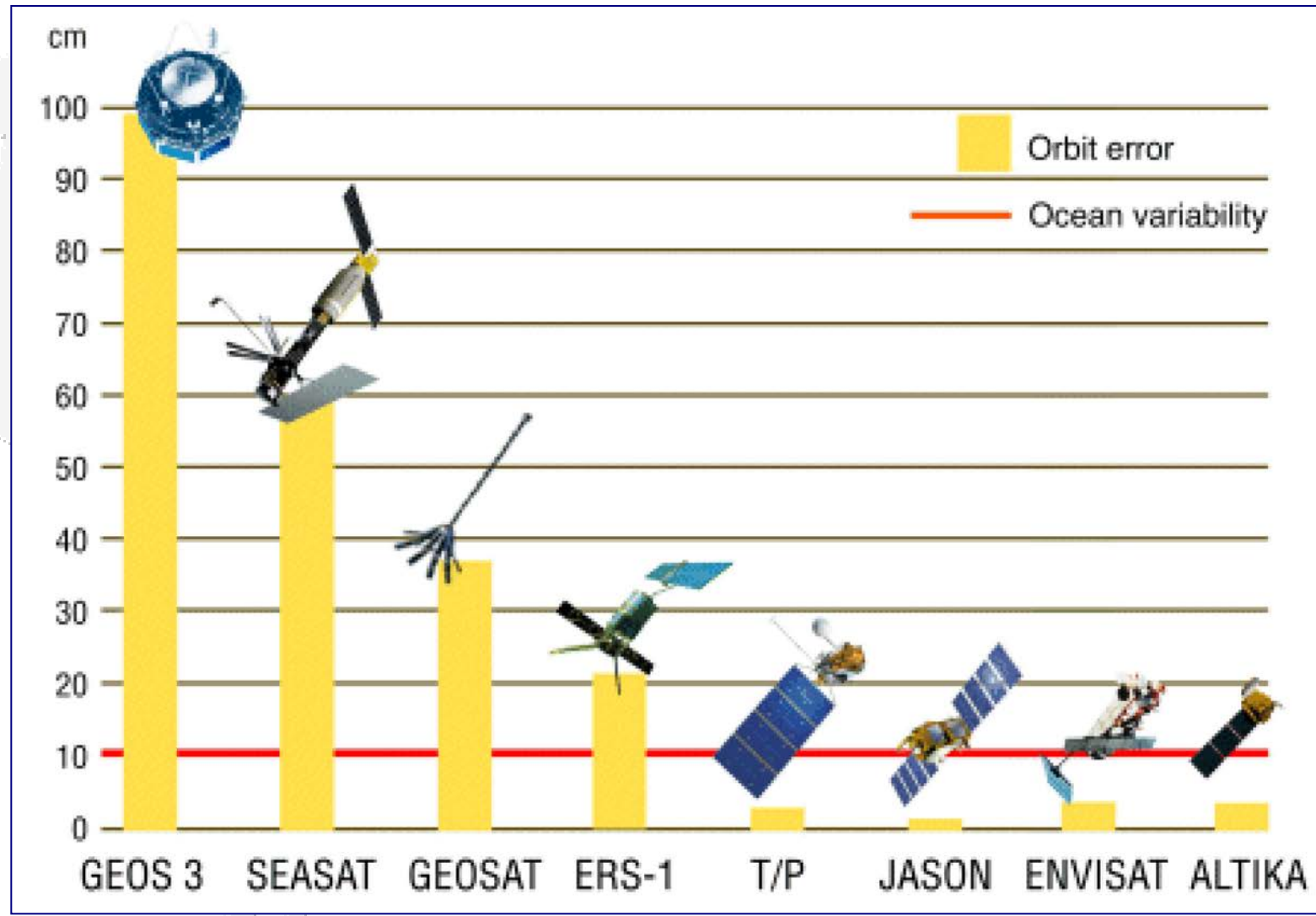


20 July — 1 August 2014,
Tver, Russian Federation

Tver State University.



Error Budget for altimetric missions



Joint COSPAR and WMO Capacity Building Workshop
«Satellite remote sensing, water cycle and climate change»

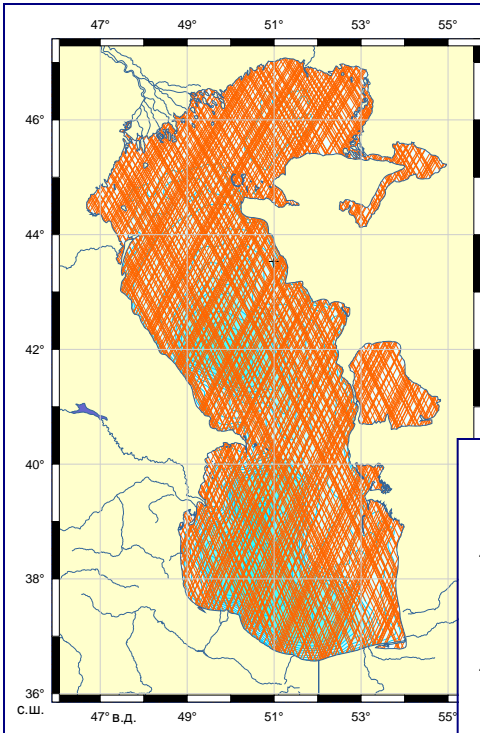
© 2014, S.A. Lebedev, GC RAS, SRI RAS



20 July — 1 August 2014,
Tver, Russian Federation
Tver State University.

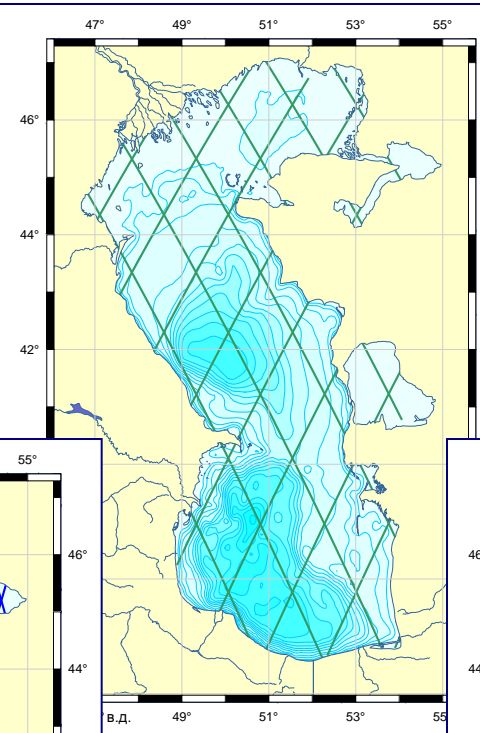


Geodetic and Exact Repeat Mission

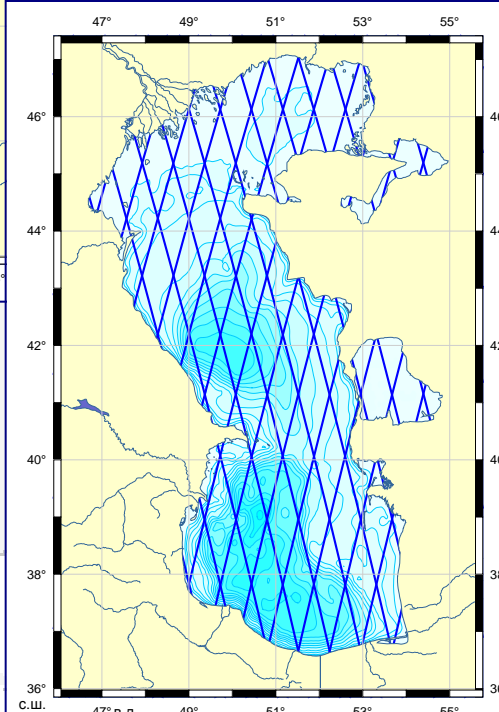


**GEOSAT
(geodetic mission)**

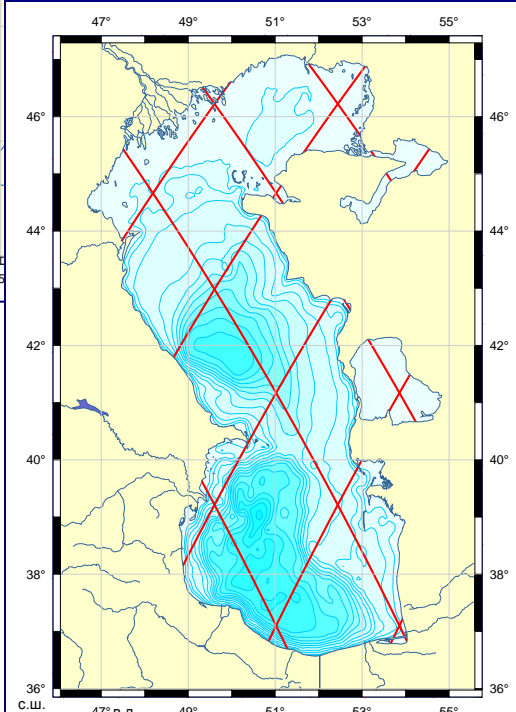
**ERS 1/2 и
ENVISAT,
SARAL
(35 days)**



**TOPEX/Poseidon и
Jason 1/2 (10 days)**



**GEOSAT и
GFO 1
(17 days)**



**20 July — 1 August 2014,
Tver, Russian Federation**

Tver State University.



**Joint COSPAR and WMO Capacity Building workshop
«Satellite remote sensing, water cycle and climate change»**

© 2014, S.A. Lebedev, GC RAS, SRI RAS





**Спасибо за
внимание**

**Thank you for your
attention**



**Joint COSPAR and WMO Capacity Building Workshop
«Satellite remote sensing, water cycle and climate change»**



**20 July — 1 August 2014,
Tver, Russian Federation**
Tver State University.

